Optimizing the Shock Wave-to-Vortex Power Ratio at the End of a Waveguide

Henri Malinen
Electronics Research Lab, Department of Physics
University of Helsinki
Helsinki, Finland
henri.malinen@helsinki.fi

Jesse Heikkilä
Electronics Research Lab, Department of Physics
University of Helsinki
Helsinki, Finland

Peetu Ihalainen
Electronics Research Lab, Department of Physics
University of Helsinki
Helsinki, Finland

Daniel Veira Canle
Electronics Research Lab, Department of Physics
University of Helsinki
Helsinki, Finland

Antti Kontiola
University of Helsinki
Helsinki, Finland

Ari Salmi
Electronics Research Lab, Department of Physics
University of Helsinki
Helsinki, Finland

Edward Hæggström
Electronics Research Lab, Department of Physics
University of Helsinki
Helsinki, Finland

Shock waves and vortices are two different ways of transferring acoustic energy to a sample in a contactless manner. This study aims at understanding the power ratio between shock waves and vortices as they exit a wave guide. Diverging tube ends increased the ratio, whereas converging ones decreased it. The power ratios were 0.1 to 9.8. Schlieren imaging was used to quantify the power-ratios. Altering the curvature at the end of the waveguide allows optimization of the shock wave-to-vortex power ratio at the end of a waveguide.

Keywords—shock wave, vortex, waveguide

I. Introduction

Shock waves are perturbations that propagate faster than the speed of sound in a medium. Their characteristic sharp pressure profile and high propagation velocity make them suitable as a broadband mechanical actuation method. Shock waves are used in medicine disintegrate kidney stones and in the industry e.g. to clean silicon wafers. [1,2]

Propagating shock waves generate vorticity when they encounter a widening [3], such as the end of a waveguide. This is due to the change in velocity along the radial direction. Optimizing the end of a waveguide to produce a certain (power) ratio of the shock wave and vortex is sometimes desirable. It allows choosing between a fast propagating excitation (shock wave) and one that deposits a large momentum (vortex).

We studied this power ratio. Custom 3D-printed structures were used to alter the relative acoustic power of the shock wave and the vortex at the end of a waveguide. The ends were: a tubular end A, diverging ends B and C, converging ends D and E, and two ends F and G combining diverging and converging curvatures (Fig. 1).

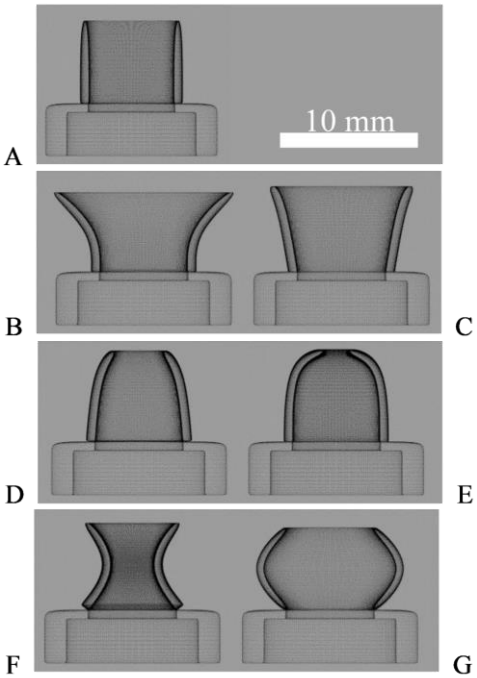

Fig. 1. Wireframe sketches of the different ends of the waveguide

II. Measurements

Shock waves were generated by discharging a 220 nF capacitor charged to 1.8 kV between tungsten electrodes. The electric discharge was inside a 3D-printed chamber that was coupled to a tubular, constant cross-section, waveguide. The inner diameter of the waveguide was 6.5 mm.

Schlieren imaging was used to quantify the acoustic power ratios at the end of the waveguide. The schlieren setup was a

compact and linear, lens-based system with straight dual-field lenses with 20 cm focal distance, a green led (Led Engin LZ1-00G102) and a camera (IDS UI-3480CP).

The end of the waveguide was modified with custom 3D-printed ends (Fig. 1). The diverging ends provide a smooth transition out of the waveguide, limiting the vorticity. The converging ends create a positive velocity gradient inside the waveguide, which generates more vorticity.

Acoustic power is defined as:

$$P = p^2 AZ \qquad (1)$$

where P is the acoustic power, p the pressure, A the cross-sectional area and Z the acoustic impedance of the medium.

In schlieren images, the deflection of the light beam depends on the integral of the change in refractive index, caused by pressure, along the imaging axis.

$$\theta = \frac{Z}{n_0}\frac{\partial n}{\partial y} \qquad (2)$$

where θ is the deflection angle, n_0 the bulk refractive index of the medium, n the refractive index, R the specific gas constant, and T the temperature. The brightness of each individual pixel is related to this deflection. The relation is linear, assuming small deflection angles.

The Gladstone-Dale equation relates the refractive index to density, and using the ideal gas law, the density can be related to the pressure:

$$\rho = \kappa(n+1), \quad p = \rho RT \qquad (3,4)$$

where ρ is the density, κ the Gladstone-Dale constant, n the refractive index, R the specific gas constant, and T the temperature.

III. Results

Schlieren images (Fig. 2) were analyzed by integrating over the square of the brightness values inside the area of -3 dB in pressure and by multiplying by the cross-sectional area. Analysis of the relative acoustic power of the shock wave and the vortex was done over a span of 45 µs (Fig. 3, Fig. 4).

$$\frac{P_{SW}}{P_V} = \frac{p_{SW}^2 A_{SW}}{p_V^2 A_V} \qquad (5)$$

The diverging ends (B, C) created less vorticity compared to the tubular end. The converging ends (D, E) created more vortices that were confined and propagated rapidly. The size of the vortex is determined by the diameter of the opening, which was small in the converging ends. The waveguide ends (F, G) generated comparable power ratios to the tubular end A.

The shock wave-to-vortex power ratio (5) ranged between 9.8 (for the diverging end C) and 0.1 (converging end D). The average pressure at the end of the converging ends was lower than that of the diverging and tubular ends.

The median peak pressure and the median acoustic power of the shock wave and vortex over the 45 µs were investigated to compare the tube ends (Fig. 5, Fig. 6). The curvature changed the proportions of the shock wave and vortex pressure. The tubular waveguide end A provided the highest total acoustic power followed by the converging ends. The lower total power with the diverging ends is due to the weakened vortex from the diverging end and from the fact that the power of the shock wave is reduced due to increased geometric spreading.

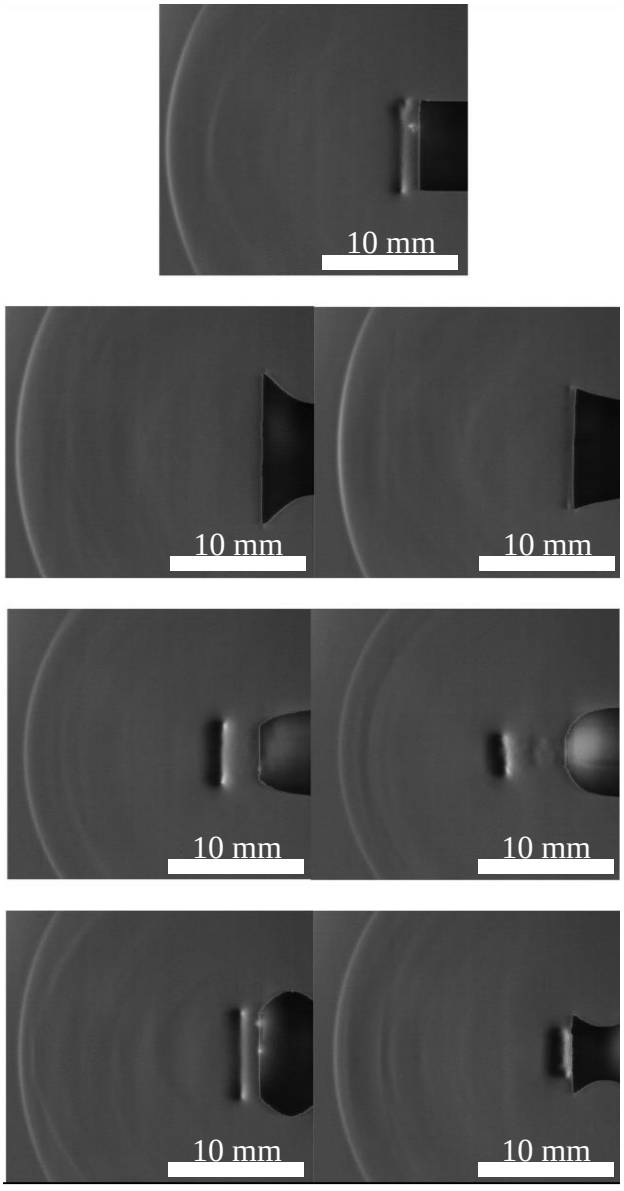

Fig. 2. Schlieren images from the waveguides showing a shock wave and a vortex at t=33 µs.

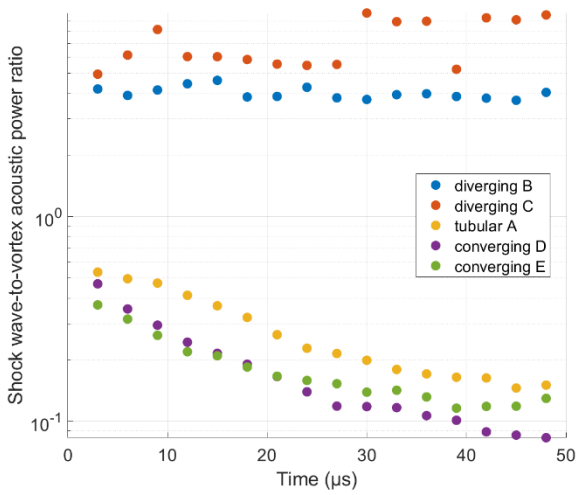

Fig. 3. Time evolution of the shock wave-to-vortex acoustic power ratio from the waveguide ends.

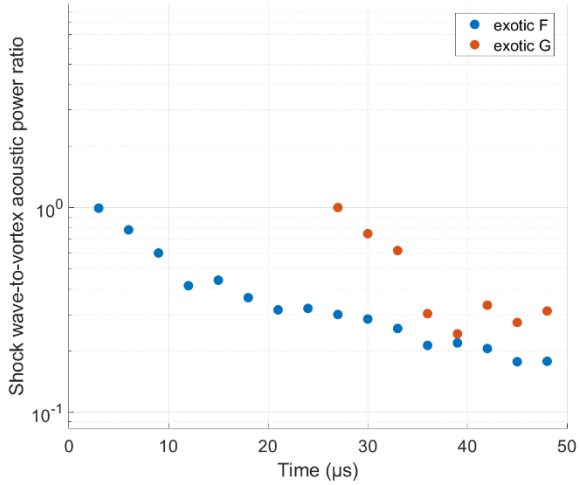

Fig. 4. Time evolution of the shock wave-to-vortex acoustic power ratio from the wave guide ends F and G. The vortex exits the exotic end G at t=27μs.

IV. Discussion

The results show that altering the direction and the radius of the curvature of the end of a waveguide modifies the shock wave-to-vortex acoustic power ratio. Diverging ends of the waveguide increase the ratio, whereas converging ends decrease it. There seems to be a sweet spot in the curvature with larger effect on the acoustic power ratio, since the ratio was higher with the smaller radii of curvature ends C and D.

The diverging ends allowed for a higher median pressure of the shock wave compared to a tubular end. The converging ends decreased the pressure of the vortex, but the effect on the shock wave was greater, allowing for a lower shock wave-to-vortex power ratio.

Combining the diverging and converging curvatures did not provide interesting results other than the delayed vortex from the tube end G.

The shock wave-to-vortex power ratio could be studied as a function of the radius of curvature of the opening either by experiments or perhaps rather with FEM simulations.

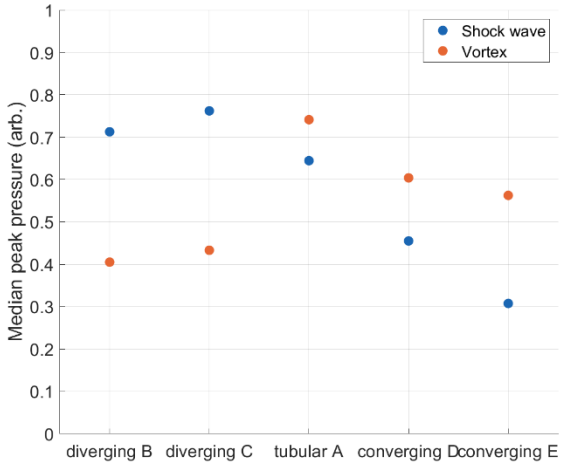

Fig. 5. Normalized median peak pressure over the 45 μs from the different waveguides.

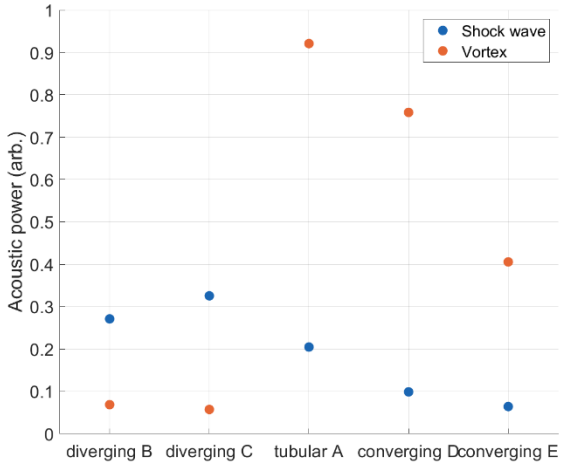

Fig. 6. Normalized median acoustic power over the 45 μs from different waveguides.

V. Conclusions

By modifying the curvature of the opening makes it is possible to change the shock wave-to-vortex power ratio at the end of a waveguide.

Acknowledgment

Thank you, Mr. Joni Mäkinen, for support in the writing process.

References

[1] Jagadeesh, G. (2008). Industrial applications of shock waves. Proceedings of the Institution of Mechanical Engineers, Part G: Journal of Aerospace Engineering, 222(5), 575-583.

[2] Sackmann, M., Delius, M., Sauerbruch, T., Holl, J., Weber, W., Ippisch, E., ... & Paumgartner, G. (1988). Shock-wave lithotripsy of gallbladder stones. New England journal of medicine, 318(7), 393-397.

[3] Sun, M., & Takayama, K. (2003). Vorticity production in shock diffraction. Journal of Fluid Mechanics, 478, 237-256.